Transport Characteristics of Suspensions: Part VI. Minimum Transport Velocity for Large Particle Size Suspensions in Round Horizontal Pipes

DAVID G. THOMAS

Cambridge University, Cambridge, England

The minimum transport velocity (defined as the mean-stream velocity required to prevent the accumulation of a layer of stationary or sliding particles on the bottom of a horizontal conduit) was determined in a 1-in. pipe for an aqueous suspension of glass beads using glass beads having mean diameters of 78 and 310 μ.

The results of the present study were combined with prior pneumatic- and hydraulic-transport data for air and water suspensions to give a unique minimum-transport relation, valid for particles larger than the thickness of the laminar sublayer, that is for particles which are immersed in the buffer layer or which extend into the turbulent core when resting on the pipe wall. The correlation showed that the ratio of particle settling velocity to friction velocity at the minimum transport condition was a function of particle Reynolds number, pipe Reynolds number, and the relative density ratio of particle to fluid. The results of the correlation suggest that a single mechanism is responsible for the initiation of particle transport throughout the range of conditions covered. This mechanism may be identified with Bernoulli forces due to instantaneous velocity differences accompanying turbulent fluctuations and largely confined to the buffer layer.

In the second paper (*1*) in this series the minimum transport velocity was determined for flocculated particles which were both smaller than the thickness of the laminar sublayer and which settled according to Stokes's law. For velocities greater than the minimum transport velocity these particles were sufficiently small to be distributed symmetrically throughout the conduit cross section by the action of turbulent eddies.

Correlation of the data showed that for dilute suspensions the minimum transport condition was given by the expression

$$U_t/u_o^* = 0.0083\ (D_p\, u_o^*\, \rho/\mu)^{2.01} \quad (1)$$

An analysis of the forces exerted on particles in the above size range resting on the bottom of the conduit showed that both Bernoulli forces and the action of turbulent fluctuations which penetrate the laminar sublayer gave substantially the same functional relationship as Equation (1).

Hydraulic and pneumatic transport of solids has found wide application in such diverse fields as the movement of hundreds of thousands of pounds of coal per hour from the pithead to steam power plants (*2*), the conveyance of catalyst in fluidized-bed chemical reactors (*3*), and the movement of fertile material through the blanket region of homogeneous nuclear reactors (*4*). These applications frequently involve particles considerably larger then the 60- to 100-μ range which is the upper limit for Equation (1) with water. Therefore it was desirable to extend the correlation to large size particles and also to verify the applicability of Equation (1) to nonflocculated particles smaller than the thickness of the laminar sublayer. An empirical-analytical approach similar to that used in the previous paper was adopted because this provided a suitable framework for the analysis of the forces responsible for particle transport and also because it permitted the incorporation of the substantial body of information in the literature which pertains to the transport of solids. The complexity of the problem was reduced somewhat by dividing it into two parts: (1) the determination of the form of the minimum transport correlation for the limiting case of infinite dilution (that is a single particle resting on the bottom of the conduit), and (2) the determination of the concentration dependence for the minimum transport correlation.

David Thomas is on leave from Oak Ridge National Laboratory, Oak Ridge, Tennessee.

BASIC CONCEPTS

The minimum transport velocity is the mean-stream velocity required to prevent the accumulation of a layer of stationary or sliding particles on the bottom of a round horizontal conduit. The minimum transport velocity is always sufficient to prevent longitudinal concentration gradients [that is the congregation of particles into islands or mounds which slowly slide along in contact with the bottom of the pipe (*5*)] but frequently is not sufficiently large to prevent vertical concentration gradients due to the action of gravity on the particulate matter.

The distinction between sliding bed and suspension flow was drawn by Blatch (*6*) in 1906, but perhaps more significant was her observation (based on visual inspection of flow regimes by means of glass inserts in the pipe) that the minimum transport velocity coincided with the minimum in a plot of pressure drop vs. velocity. This observation on the minimum transport condition has been amply verified for aqueous suspensions by subsequent investigators (*7* to *10*). However Zenz (*3*) has warned that care must be used in interpreting data for gas-solid systems since two markedly different values of the pressure drop may be obtained in the immediate vicinity of the minimum transport velocity. The lower value of the pressure drop is found at velocities slightly greater than the minimum transport velocity and corresponds to flow with no deposit on the pipe walls. The larger value of the pressure drop is found at velocities slightly smaller than the minimum transport velocity and corresponds to flow above a settled layer. Therefore the minimum recorded value of the pressure drop must be used as the minimum transport condition when correlating data from the literature in the absence of direct observation.

Flow Regimes

In discussing suspension transport phenomena it is useful to separate the problem into different flow regimes depending on the distribution of particles in the pipe or on the nature of the flow around the particles.

Particle Distribution. Extensive investigations (*11*) have shown that the major factor affecting the vertical distribution of suspended solids in a flowing stream is the ratio of the terminal settling velocity to the friction velocity (U_t/u_w^*). All expressions have the form

$$c_2/c_1 = \psi\ (Z_2/Z_1)^{-U_t/\kappa u_w^*} \quad (2)$$

and are based on the simple assumption that settling due to gravity is balanced by the upward transport due to turbulence. In Equation (2) c_1 and c_2 are the concentrations at elevations Z_1 and Z_2, respectively; the coefficient κ is commonly (*12*) considered a universal constant for the flow of homogeneous, Newtonian fluids with a value

of 0.4. However sediment transport data (13) indicate that it may have a value as low as 0.19 in two-phase flow. The friction velocity is given by

$$u_w^* = \sqrt{g_c \tau_w/\rho_m} = \sqrt{g_c D\, \Delta p/4\, \rho_m L} \quad (3)$$

and is related to the mean-stream velocity in circular conduits by (25)

$$U/u_w^* = 5 \log N_{Re} - 3.90 \quad (4)$$

The terminal settling velocity is the settling rate of a single particle in the fluid medium.

The selection of a particular value of the ratio U_t/u_w^* as a point of division into different flow regimes is somewhat arbitrary since the vertical concentration gradient varies continuously with U_t/u_w^*. With this limitation a value of $U_t/u_w^* = 0.2$ represents a convenient measure of whether the solids are being transported in suspension or as a concentrated layer moving through the lower portion of the pipe. For values less than 0.2 the particulate phase is transported substantially in suspension; for values greater than 0.2 the particulate phase is transported predominantly in a layer along the bottom of the pipe. More quantitatively the value of 0.2, when inserted in Equation (2), gives a concentration ratio at elevation $Z_2/D = 0.88$ and $Z_1/D = 0.12$ of $c_2/c_1 = 1/e$. The value of $U_t/u_w^* = 0.2$ is estimated to be within 10% of the criterion given by Durand (7) for suspended flow in sand-water systems under normal sediment transport conditions, namely that suspended flow would be expected for particle sizes less than 200 μ. This criterion based on particulate size alone is of course less general than the one given above.

Particle Flow Regimes. The nature of the flow around a particle as it settles toward the bottom of a conduit may be represented on a plot of U_t/u_o^* vs. $D_p u_o^* \rho/\mu$ [for example Equation (1)] by lines of constant particle Reynolds number, $(D_p u_o^* \rho/\mu)$ $(U_t/u_o^*) = N_{Re}$ = constant. The equations relating particle and fluid characteristics to the terminal settling velocity are readily available (14) and will not be repeated here. The demarcation between the different settling-rate expressions is given by:

Stokes's law (laminar flow):

$$N_{Re} < 1 \quad (5)$$

Intermediate law (transition):

$$1 < N_{Re} < 500 \quad (6)$$

Newton's law (turbulent flow):

$$N_{Re} > 500 \quad (7)$$

The lines separating these flow regimes

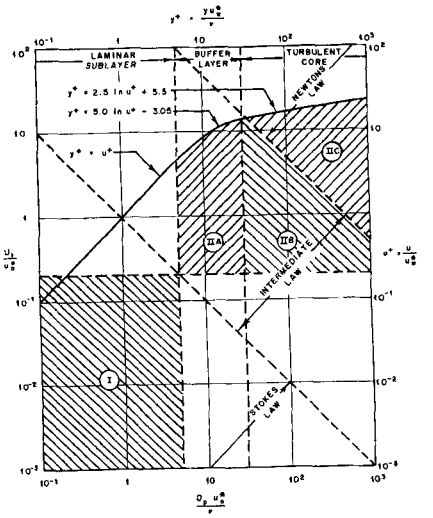

Fig. 1. Flow regime classification for minimum transport correlation.

are identified in Figure 1 together with the line for $U_t/u_w^* = 0.2$, which is the dividing line for suspension flow and for flow predominantly in a layer along the bottom of the pipe.

Finally, by considering the case of a particle momentarily in contact with the pipe wall, one can establish whether the particle is immersed in the laminar sublayer or whether the particle projects into the buffer region or into the turbulent core. Von Karman (15) defined the thickness of these layers in terms of the dimensionless parameter $y^+ = y u_w^* \rho/\mu$:

Laminar sublayer: $y^+ < 5$ (8)

Buffer layer: $5 < y^+ < 30$ (9)

Turbulent core: $y^+ > 30$ (10)

These limits are shown on Figure 1 with the same value for the co-ordinates as used for the minimum transport correlation, thus giving the comparison directly. The universal velocity profile defined by von Karman is also shown in the upper portion of Figure 1 and may be considered as the maximum forward velocity that can be acquired by a particle when being transported upwards from the bottom of the pipe.

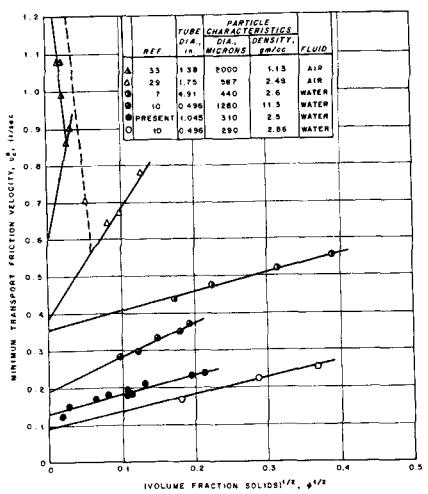

Fig. 2. Effect of concentration on friction velocity at the minimum transport condition.

The definitions given above divide the minimum transport problems for the limiting case of infinite dilution into two major flow regimes, one of which can be subdivided into three regions (see Figure 1):

1. Flow with particles predominantly in suspension and particles which are smaller than the thickness of the laminar sublayer [Equation (8)] and which settle according to Stokes's law [Equation (5)], (flow regime I).
2. Flow with particles transported predominantly in lower portion of pipe:

(a) Particles which are smaller than the thickness of the buffer layer [Equation (9)] and which settle according to the intermediate law [Equation (6)], (flow regime IIA).

(b) Particles which are larger than the thickness of the buffer layer [Equation (10)] and which settle according to the intermediate law [Equation (6)], (flow regime IIB).

(c) Particles which are larger than the thickness of the buffer layer [Equation (10)] and which settle according to Newton's law [Equation (7)], (flow regime IIC).

Flow regime I was treated in the second paper in this series (1), but this paper is concerned primarily with regime II, although new data for nonflocculated suspensions are also presented to provide continuity with the previous paper.

Particle Transport Mechanism

By definition the minimum transport velocity occurs when the particles cease to slide along the bottom of the pipe but are transported by saltation. As described by Bagnold (16) there is a pronounced difference in saltation characteristics depending on whether the working fluid is air or water. With water the particles do not bounce more than a few particle diameters above the pipe wall, whereas with air particles may bounce from 100 to 1,000 particle diameters. Under some circumstances this means that particles bounce from wall to wall as they are transported along the pipe (17). Bagnold (16) has shown that this difference is primarily a function of the ratio of particle density to fluid density and may be thought of as due to the difference in speed with which grains strike the wall in the two different fluids. Bagnold also showed that if there was a deposit of particles on the bottom of the pipe in the air-suspension studies, the momentum of a returning particle was sufficient to produce a distinct splash

TABLE 1. RANGE OF VARIABLES INCLUDED IN MINIMUM TRANSPORT CORRELATION FOR FLOW REGIME II

	Water	Air
Pipe, diameter, D, in.	0.496 to 32	0.62 to 1.75
Particle diameter, D_p, μ	190 to 38,100	97 to 2,000
Settling velocity, ft./sec.	0.067 to 2.07	1.35 to 23.0
Particle density, g./cc.	1.3 to 11.3	1.08 to 2.65
Fluid density, g./cc.	0.98 to 1.0	0.0012 to 0.0029
Viscosity, centipoise	0.54 to 1.5	0.018
Friction velocity, ft./sec.	0.08 to 0.54	1.04 to 2.7
D_p/D	0.00033 to 0.25	0.0062 to 0.057

of particles, thus enhancing materially the ability of the air stream to transport solids. The problem of resolving the transport mechanisms is further complicated by the poor understanding of such factors as the effect of velocity gradients on the rotation of particles (*18, 19*) and the effect of turbulent fluctuations on the dynamics of a freely moving body (*20*).

Nevertheless certain forces may be identified, among which are:

1. Gravitational forces (*14*) causing particles to settle.
2. Bernoulli forces (*20*) caused by the mean velocity gradient across the particle and by instantaneous velocity differences accompanying turbulent fluctuations.
3. Forces caused by the spin of the particles (*18, 19*) which give rise to the Magnus effect.
4. Viscous drag caused by the action of the mean velocity on the particle (*24*).
5. Frictional force between the particle and the wall as the particle bounces (*35*).

The particular forces relevant to a discussion of the minimum transport condition are those acting opposite to gravity since by definition there must be sufficient lift on a particle to impart a bouncing motion. The only forces from the list given above which need to be considered are the Bernoulli forces and those accompanying the Magnus effect. Torobin and Gauvin (*18*) have reviewed the data for spinning particles and concluded that under most circumstances the Magnus effect would not contribute appreciably to particle entrainment. Irmay (*20*) has made a detailed study of particle trajectories and has shown that there is a mean acceleration reaching 15 g_L and more in the buffer layer [Equation (9)] directed upstream and somewhat toward the axis. These large forces on the particles are due to instantaneous accelerations accompanying the turbulent fluctuation of the fluid medium and apparently are of primary importance in the turbulent transport of particles.

Since measurement of turbulent fluctuations was beyond the scope of the present paper, an alternative correlation procedure was required. As in the previous paper (*1*) advantage is taken of the fact that Laufer (*21*) showed that the turbulent fluctuations at any given radial position are proportional to the friction velocity essentially independent of the Reynolds number. If the particle terminal settling velocity is taken as a measure of the gravitational forces, the friction velocity may be taken as a measure of the radial forces on a particle, and the ratio of these two terms U_t/u_o^* will be considered as one of the primary factors in the subsequent correlation. Results of turbulence studies (*18, 21*) suggest that this ratio will be a function of both a particle Reynolds number and a pipe Reynolds number. Other factors which may be important will be discussed in a later section.

EQUIPMENT AND PROCEDURE

The equipment and procedure were described previously (*1*) Significant features were the loop system having a weigh tank for determining flow rate and a 40-ft. section of 1.045-in. diam. pipe. The last 10 ft. of the section consisted of glass pipe where the minimum transport condition was determined visually. The suspension was circulated by means of a pump with a variable speed drive; a bypass line around the test section gave additional flexibility in adjusting the velocity.

All the solids in the system were suspended completely before the start of any minimum transport velocity determination. The mean velocity was then lowered until the first sediment was observed sliding along the bottom of the conduit. The velocity was then increased to resuspend the sediment and lowered again to a value slightly higher than when the sliding bed was observed. This procedure was followed until the system had operated for at least 30 min. with no sliding bed and with the suspension being transported by saltation. The mean-stream velocity for this condition was defined as the minimum transport velocity and was reproducible to within ±5%.

The particulate phase used in this study consisted of two different sizes of commercially available glass beads: −140, +270 mesh with a mean diameter of 78μ, and −40, +70 mesh with a mean diameter of 310μ. The concentration was varied from 10^{-4} to 6×10^{-2} volume fraction solids. Concentrations in this range were determined by collecting a 1-liter sample of suspension from the discharge to the weigh tank and evaporating to dryness. Emphasis was placed on the dilute concentrations in order to verify the concentration dependence deduced from literature data which usually were more concentrated with a range of 10^{-2} to 4×10^{-1} volume fraction solids.

Mean-settling rates were determined from hindered-settling measurements extrapolated to zero concentration with the relation developed by Steinour (*22*); these settling rates corresponded within experimental error to the value calculated (*14*) from the mean diameter. If settling rates were not reported in the literature, they were calculated with the procedure outlined by Lapple (*14*), and when necessary a correction for nonsphericity was applied based on the extensive data of Richards (*23*).

EXPERIMENTAL RESULTS

Typical results for a variety of different air and water suspensions are shown in Figure 2 as the friction velocity at the minimum transport condition vs. the square root of the volume fraction solids. The data for the present study were obtained by direct observation through the glass pipe walls, but the data from the literature represent the minimum in the plot of pressure gradient against velocity, the value commonly accepted (*6* to *9*) as corresponding to the minimum transport velocity. Two facts are immediately obvious from Figure 2: the data for gas-solid systems exhibited a pronounced minimum in the friction velocity, whereas the data for liquid-solid systems followed a straight-line relationship:

$$u_o^* - u_o^* = K\phi^{1/2} \qquad (11)$$

The term u_o^* is just that required for the correlation according to the scheme outlined above.

The situation in gas-solids systems is not as clear because the data are quite limited; nevertheless available data are qualitatively similar and appear to be entirely consistent with the extensive observations of Bagnold (*24*). He observed that in the absence of suspended solids very large friction velocities were required to initiate particle flow. As soon as solids became suspended, the friction velocity required to maintain flow was materially reduced because of the large amounts of energy picked up by particles from the high-velocity portion of the stream and transmitted to the wall region as the particles collided with the wall. From this brief description it is clear that the data to the left of the minimum in Figure 2 are those to be extrapolated to zero concentration to obtain u_o^* for gas-solid suspensions; that is the minimum

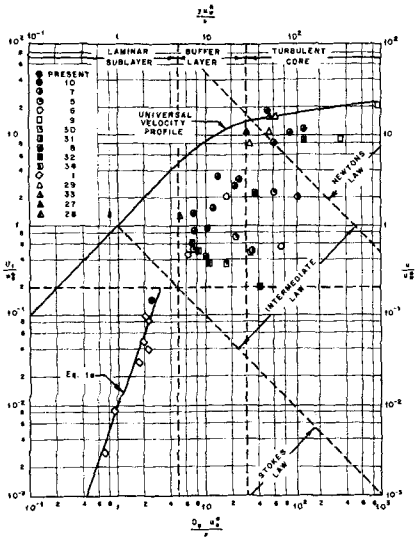

Fig. 3. Experimental results classified by flow regimes.

transport correlation is primarily concerned with fluid-particle interactions, not particle-particle interactions.

The results of the present study, as well as extensive data from the literature, are shown in Figure 3 within the same framework used in Figure 1 to define different flow regimes. (Note that triangular-shaped points are used for all gas-solid data.)

The only new result in flow regime I is that of the present study with nonflocculated glass beads with a mean diameter of 78 μ. It is in good agreement with the other regime I results, and a least-squares analysis gives

$$U_t/u_o^* = 0.010\ (D_p\, u_o^*\, \rho/\mu)^{2.71} \quad (1a)$$

The exponent in Equation (1*a*) is in better agreement with that derived from Bernoulli's theorem than with the exponent derived from penetration theory (*1*) (that is, 3 and 2, respectively); however the value of the numerical coefficient is somewhat lower than predicted by either analysis (0.0104 and 0.0154, respectively).

The range of variables covered by the flow regime II data are shown in Table 1. When one considers the ranges for both air and water, there is at least a tenfold variation in all of the factors listed, and if the particle density ratio $(\rho_p - \rho)/\rho$ rather than particle density were considered, then a greater than thirtyfold variation of all factors would be represented. The scatter of the flow regime II data of Figure 3 shows that the analysis for particles smaller than the thickness of the laminar sublayer (flow regime I) is no longer adequate and that additional parameters must be considered in order to obtain a satisfactory correlation.

CORRELATION OF RESULTS

Minimum Transport Condition

Conventional dimensional analysis showed that the minimum transport condition for the limiting case of infinite dilution could be expressed by the relation

$$U_t/u_o^* = k\,\{(D_p\, u_o^*/\nu)^a\ (D\, u_o^*/\nu)^b\ [(\rho_p - \rho)/\rho]^c\} \quad (12)$$

with the constant k and the exponents a, b, and c to be determined experimentally. In addition to the Reynolds numbers mentioned in the mechanism section, the one new variable is the term $[(\rho_p - \rho)/\rho]$. Note also that in Equation (12) the gravitational terms are incorporated in the terminal settling velocity and the pressure gradient is incorporated in the friction velocity [Equations (3) and (4)].

The results of the analysis of the minimum transport data for flow regime II are shown graphically in Figure 4 and are given by Equation (12) when $k = 4.90$, $a = 1$, $b = -0.60$, and $c = 0.23$. With these values the data are correlated with a mean deviation of +26 and −17% and a maximum deviation of +55 and −38%.

Concentration Dependence

The friction velocity at the minimum transport condition was found to be proportional to the square root of the volume fraction solids for all concentrated gas and liquid suspensions as illustrated in Figure 2 and Equation (11). The constants of proportionality K obtained by application of Equation (11) to the gas and liquid suspension data are shown in Figure 5 plotted as K/u_o^* vs. U_t/u_o^*. For flow regime II the data are fitted by the equation

$$K/u_o^* = 2.8\ (U_t/u_o^*)^{1/3} \quad (13)$$

with a mean deviation of +28% and −18%. If one combines Equation (13) and Equation (11), the complete expression for the concentration dependence of the minimum transport correlation is

$$\frac{u_c^* - u_o^*}{u_o^*} = 2.8\left(\frac{U_t}{u_o^*}\right)^{1/3} \phi^{1/2} \quad (14)$$

Care must be exercised in using both Equations (12) and (14) with data for gas-solid suspensions because of the minimum observed in the plots of friction velocity vs. concentration (Figure 2). Although there were insufficient data to completely specify the nature of the minimum, some qualitative observations may be made:

1. In each of the gas-solid references cited, sufficient data were included to definitely establish the existence of the minimum.

2. In only one case was there enough data to accurately locate the curve on both sides of the minimum. In other cases the uncertainty in the location of one arm of the curve was estimated; this uncertainty is shown by the wings on those points.

3. The friction velocity for the gas-solid data used in Equation (12) was the intercept of the dilute portion of the curve, whereas the friction velocity for the gas-solid data used in Equation (14) was designated as $u^*_{c,o}$.

4. As shown in Figure 5 the ratio $(u^*_o/u^*_{c,o})$ may be considered a constant within rather broad limits with an approximate value of 4.4 (*see* Table 2).

The increase in slope of the curve at the transition from regime II to regime I (Figure 5) is consistent with the previous observation (*1*) that the minimum transport friction velocity was essentially independent of concentration for all regime I data. In other words a value of $K/u_o^* = 1$ corresponded roughly to an increase of only 10% in the friction velocity as the concentration was increased from 0 to 0.317 volume fraction solids.

DISCUSSION OF RESULTS

Comparison of the upward forces acting on a particle resting on the bottom of a horizontal pipe showed that the primary contribution was due to Bernoulli forces arising from instan-

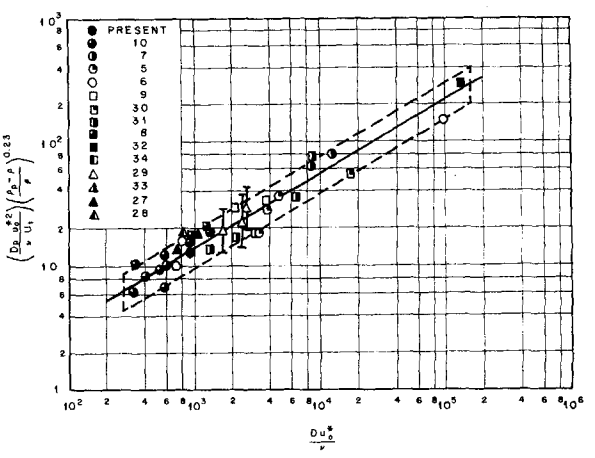

Fig. 4. Minimum transport correlation for limiting case of infinte dilution.

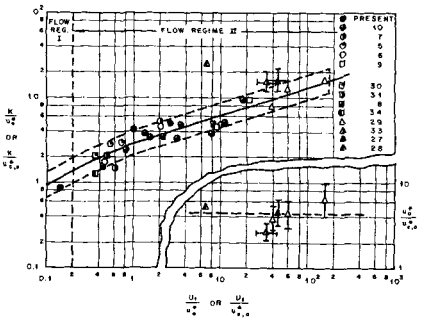

Fig. 5. Concentration correlation.

Table 2. Effect of Particle Characteristics on Ratio of Minimum Transport Friction Velocities for Gas-Solid Suspensions for the Limiting Case of Infinite Dilution

Material	Particle characteristics Diameter, D_p, μ	ρ_p, g./cc.	$\frac{D}{D_p}$	ϕ_c, volume fraction solids	$\frac{u_o^*}{u_{c,o}^*}$
Rape seed (29)	1,675	1.08	26.5	0.018	6.4
Glass beads (29)	587	2.49	75.7	0.004	4.3
Sand (29)	930	2.64	47.8	0.004	3.7
Cress seed (27)	1,060	1.17	24.0	0.031	4.4
Mustard seed (33)	2,000	1.13	17.5	0.0007	2.6
Glass beads (28)	97	2.6	162.0	0.014	5.2

taneous velocity differences accompanying turbulent fluctuations. Irmay (*20*) showed that these forces were localized in the buffer layer and that they produced a mean acceleration reaching 15 g_L and more. Since measurement of the turbulent fluctuations was beyond the scope of the present study, advantage was taken of the proportionality between the turbulent fluctuations and the friction velocity (*21*) to obtain an estimate of the magnitude of the fluctuations. On this basis the ratio U_t/u_o^* may be considered as a measure of the tendency of gravitational forces to overcome the action of turbulent fluctuations. This ratio has also been shown (*11*) to be the principal factor affecting the distribution of solids in a flowing stream [Equation (2)]. At this point it was necessary to resort to dimensional analysis and experiment to obtain the functional relationship between the term U_t/u_o^*, the system dimensions, and operating variables. The problem was divided into the limiting case of the minimum transport conditions at infinite dilutions and the concentration dependence. The final results were

$$U_t/u_o^* = 4.90\ (D_p u_o^*/\nu)$$
$$(\nu/D\,u_o^*)^{0.60}\,[(\rho_p - \rho)/\rho]^{0.23} \quad (15)$$

and

$$u_c^*/u_o^* = 1 + 2.8\ (U_t/u_o^*)^{1/3}\,\phi^{1/2} \quad (16)$$

The gas-solid suspension data were in good agreement with the liquid-solid suspension data, although additional information is required on the characteristics of gas-solids flow in order to complete the details of the concentration dependence.

The fact that a simple functional relationship was obtained for the combined data for flow regimes II (*a*), II (*b*), and III (*c*) which covered the very wide range of variables listed in Table 1 indicate that in all probability one mechanism is controlling throughout the entire range. This supports the results presented by Irmay (*20*) and Kline and Runstadler (*26*) which show that the large mean accelerations and forces which act in a particle are largely limited to the buffer layer defined by Equation (9). In other words, although individual particles may have quite different trajectories in the different flow regimes, the initial upward impulse is apparently localized in the buffer layer resulting in the single straight-line relation shown in Figure 4.

ACKNOWLEDGMENT

The data were obtained at Oak Ridge National Laboratory, and the paper was written during the tenure as a National Science Foundation Senior Postdoctoral Fellow at Cambridge University; sincere thanks are expressed for the opportunity thus afforded.

NOTATION

a,b,c = exponents, dimensionless
c_1,c_2 = concentration, particles per unit volume at positions 1 and 2
D = tube diameter, ft.
D_p = particle diameter, ft.
e = 2.718 . . . .
g_c = conversion factor, (lb.-mass/lb.-force) (ft./sec.^{2})
g_L = gravitational acceleration, ft./sec.^{2}
k = coefficient, dimensionless
K = coefficient, ft./sec.
N_{Re} = Reynolds number, dimensionless
u_c^* = friction velocity at minimum transport condition (MTC), ft./sec.
u_o^* = friction velocity at MTC for limiting case of infinite dilution, ft./sec.
$u_{c,o}^*$ = friction velocity at MTC from extrapolation of concentrated gas-solid suspension data, ft./sec.
u_w^* = friction velocity, ft./sec.
u = local velocity, ft./sec.
u^+,y^+ = velocity profile co-ordinates, dimensionless
U = mean stream velocity, ft./sec.
U_t = terminal settling velocity, ft./sec.
y = distance from pipe wall, ft.
Z_1,Z_2 = vertical distance at positions 1 and 2, ft.

Greek Letters

$\Delta p/L$ = pressure gradient, lb.-force/cu. ft.
κ = coefficient, dimensionless
μ = coefficient of viscosity, lb.-mass/ft. sec.
ν = kinematic viscosity, sq. ft./sec.
ρ = fluid density, lb.-mass/cu. ft.
ρ_m = mixture density, lb.-mass/cu. ft.
ρ_p = particle density, lb.-mass/cu. ft.
τ_w = wall shear stress, lb.-force/sq. ft.
ϕ = volume fraction solids, dimensionless
ϕ_c = volume fraction solids at minimum in gas-solid suspension curve, dimensionless
ψ = function of, dimensionless

LITERATURE CITED

1. Thomas, David G., *A.I.Ch.E. Journal*, **7**, No. 3, p. 423 (1961).
2. Anon., "Russia Reveals New Coal Mine," *New York Herald Tribune Economic Review*, p. 1, Paris, France (Dec., 1960).
3. Zenz, F. A., and D. F. Othmer, "Fluidization and Fluid-Particle Systems," Reinhold, New York (1960).
4. McBride, J. P., and D. G. Thomas, "Fluid Fuel Reactors," Chap. 4, James A. Lane, H. G. McPherson, and F. Maslan, ed., Addison-Wesley, Reading, Massachusetts (1958).
5. Smith, R. A., *Trans. Inst. Chem. Engrs.*, **33**, 85 (1955).
6. Blatch, N. S., *Trans. Am. Soc. Civil Engrs.*, **57**, 400 (1906).
7. Durand, R., "Proceedings Minnesota Hydraulic Convention," Part 1, pp. 89-103 (1953).
8. Newitt, D. M., et al., *Trans. Inst. Chem. Engrs.*, **33**, 93-110 (1955).
9. Worster, R. C., and D. F. Denny, *Proc. Inst. Mech. Engrs.*, **169**, 563-573 (1955).
10. Murphy, G., D. F. Young, and R. J. Burian, *U.S. Atomic Energy Commission Rept. ISC-474* (1954).
11. Chien, Ning, *Trans. Am. Soc. Civil Engrs.*, **121**, 833 (1956).
12. Schlicting, Hermann, "Boundary Layer Theory," p. 406, Pergamon, London, England (1955).

13. Vanoni, V. A., and G. N. Nomicos, *Trans. Am. Soc. Civil Engrs.*, **125**, 1140 (1960).
14. Lapple, C. E., "Chemical Engineering Handbook," p. 1019, 3 ed., J. H. Perry, ed., McGraw-Hill, New York (1950).
15. von Karman, Theodore, *J. Aeronaut. Sci.*, **1**, 1 (1934).
16. Bagnold, R. A., *Brit. J. Appl. Phys.*, **2**, 29 (1951).
17. Adam, Otto, *Chemie-Ing.-Tech.*, **29**, 151 (1957).
18. Torobin, L. B., and W. H. Gauvin, *Can. J. Chem. Eng.*, **38**, 142 (1960).
19. Soo, S. L., and C. L. Tien, *J. Appl. Mech.*, **27**, 5 (1960).
20. Irmay, S., *J. Basic Eng.*, **82**, 961 (1960).
21. Laufer, John, *Natl. Advisory Comm. Aeronaut. 1174* (1954); see J. O. Hinze, "Turbulence," pp. 520-533, McGraw-Hill, New York (1960).
22. Steinour, H. H., *Ind. Eng. Chem.*, **36**, 618-624, 840-847, 901-907 (1944).
23. Richards, R. H., *Trans. Am. Inst. Mining Engrs.*, **38**, 210 (1907).
24. Bagnold, R. A., "The Physics of Blown Sands and Desert Dunes," Methuen, London, England (1941).
25. Taylor, G. I., *Proc. Roy. Soc.*, **A223**, 446 (1954).
26. Kline, S. J., and P. W. Runstadler, *J. Appl. Mech.*, **26**, 166 (1959).
27. Clarke, R. H., et al., *Trans. Inst. Chem. Engrs.*, **30**, 209 (1952).
28. Mehta, N. C., et al., *Ind. Eng. Chem.*, **49**, 986-992 (1957).
29. Zenz, F. A., *ibid.*, **41**, 2801 (1949).
30. Yufin, A. P., *Izvest. Akad. Nauk Usbekh SSR, Ser Tekh. Nauk*, No. 8, 1146 (1949).
31. Howard, G. W., *Trans. Am. Soc. Civil Engrs.*, **64**, 1377 (1938).
32. Silin, N. A., *Akad. Nauk URSR Kiev Dopovidi.*, **3**, 175-177 (1958).
33. Rose, H. E., and H. E. Barnacle, *The Engineer*, 898-901, 939-941 (June 14 and June 21, 1957).
34. Pogosoyan, M. G., *Gidrotekh. Stroit*, **27**, 39-42 (1958).
35. White, C. M., *Proc. Royal Soc.*, **174A**, 322-338 (1940).

Manuscript received September 26, 1961; revision received December 6,1961; paper accepted December 6, 1961. Paper presented at A.I.Ch.E. Baltimore meeting.

Steady Flow of an Oldroyd Viscoelastic Fluid in Tubes, Slits, and Narrow Annuli

MICHAEL C. WILLIAMS and R. BYRON BIRD

University of Wisconsin, Madison, Wisconsin

RHEOLOGICAL MODELS

One of the objectives of rheology is the development of generalized models to describe the mechanical behavior of classes of real liquids in a wide variety of steady and unsteady state conditions. Attempts to do this have been little more than constructions of empirical models to fit experimental data. Generalized Newtonian functions such as the power-law, Bingham, and Reiner-Philippoff functions (*1, 5, 23*) are found to describe steady flow of some materials in several simple geometries. However their use is usually restricted to a rather narrow range of steady flow conditions. Furthermore it is doubtful whether model parameters determined in one kind of viscometer would agree with those found in another type of viscometer. For example Fredrickson (*5*) found that the power-law constants obtained from tube flow data were not in general valid for axial flow in a coaxial cylindrical annulus.

A basic weakness of these generalized Newtonian models is their failure to account for elastic phenomena. Such effects have been tentatively described by functions which involve time derivatives of varied significance, as listed in Table 1. The standard linear viscoelastic models utilize only $\partial/\partial t$ and are inappropriate in situations where significant inertial forces exist. Recently several rheological models have been proposed which use more general time derivatives (see Table 1), and which are intended to combine and extend previous viscoelastic and non-Newtonian models. Some of these are shown in Table 2.* In that table each model is given in the forms $0 = F(\tau_{ik}, \epsilon_{ik})$; the terms present in the function F are indicated by denoting the constant and operator multipliers associated with them. For example the De Witt model is $\left(1 + \lambda_1 \frac{\mathcal{D}}{\mathcal{D}t}\right)\tau_{ik} + 2\eta_0 \epsilon_{ik} = 0$. The quantities $\lambda_1, \lambda_2, \kappa_1, \kappa_2, \mu_0, \mu_1, \mu_2, \nu_1, \nu_2$ are constants with dimensions of time, η is a variable viscosity (g. cm.$^{-1}$ sec.$^{-1}$), and η_0 is a zero-shear viscosity.

* See also reference *13* for an analytical comparison of several rheological models.

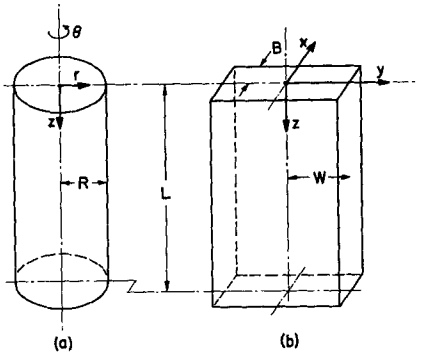

Fig. 1. (*a*) Cylindrical geometry; (*b*) plane slit geometry.

In Tables 1 and 2 Cartesian tensors are used with the usual summation convention. The quantities τ_{ik} are the components of the shear-stress tensor. The rate-of-strain tensor ϵ_{ik} and vorticity tensor ω_{ik} are defined in the usual way:

$$\epsilon_{ik} = \frac{1}{2}\left(\frac{\partial v_k}{\partial x_i} + \frac{\partial v_i}{\partial x_k}\right); \qquad \omega_{ik} = \frac{1}{2}\left(\frac{\partial v_k}{\partial x_i} - \frac{\partial v_i}{\partial x_k}\right) \quad (1)$$

Experimental testing of the newer viscoelastic models has been somewhat limited in scope. Model (*d*) has been reported to be successful in describing the response of certain dilute polymer solutions to small-amplitude oscillation (*17, 20, 30*). Model (*e*) predicts incorrectly the normal stresses present